
Pressure Field Produced by the Rapid Vaporization of a CO₂ Liquid Column

G. Ciccarelli, J. Melguizo-Gavilanes, and J.E. Shepherd

Introduction

Fundamental studies on the rapid boiling of liquids have been carried out for many years in connection with nuclear power plant severe accidents [1] and BLEVEs [2]. Reid [3, 4] proposed that if the pressurized liquid is at an initial temperature above the superheat limit temperature (also referred to as the homogeneous nucleation temperature), depressurization can lead to explosive evaporation producing a shock wave. At the superheat limit molecular fluctuations spontaneously produce nucleation sites where evaporation originates and spreads as a wave through the rest of the liquid. Small-scale experiments have been carried out to investigate evaporation wave propagation at the superheat limit by thermally heating a liquid drop to the superheat limit [5, 6] and by the rapid depressurizing of the liquid in a vertical glass tube [7–9].

Tosse et al. [10] recently performed experiments with liquid carbon dioxide (CO₂) at room temperature in a polycarbonate tube to observe the boiling process that takes place when the tube is suddenly depressurized to the atmosphere. The experiments were carried out in a polycarbonate tube as compared to the superheat limit depressurization experiments performed in Ref. [7–9] that were carried out in glass tubes. In the polycarbonate tube, heterogeneous boiling is likely initiated before the superheat limit is reached due to the availability of nucleation sites at the tube wall. High-speed front-lit photography was used to capture the global features of the CO₂ boiling, and pressure transducers were used to measure the pressure-time history at the top and bottom of the tube. For experiments where the

burst diaphragm was located at the top-end of the tube, following diaphragm rupture high-speed video showed the progression of a condensation front down through the vapor space above the liquid. Following the arrival of the condensation front at the liquid surface, the high-speed video showed two waves moving in opposite direction; the “evaporation wave” propagated at a constant velocity downward into the liquid and the “vapor-mixture interface” accelerated upward.

In the present study, the depressurization of a tube partially filled with CO₂ liquid (driver section) expanding into a similar diameter tube initially filled with nitrogen (driven section) was investigated. The main objective was to determine the effect of the CO₂ liquid phase transition on the pressure field behind the shock wave propagating in the driven section produced by the initial expansion of the CO₂ vapor and the subsequent boiling of the liquid phase CO₂ in the driver. High-resolution high-speed back-lit video was used to capture the propagation of the various phase-change fronts in the driver.

Experimental

The shock wave generation from rapid expansion driven evaporation of liquid CO₂ is studied in a vertical shock tube shown schematically in Fig. 1. The driver section, initially containing liquid CO₂ and vapor, consisted of a transparent 48 cm long, 16 mm inner-diameter polycarbonate tube positioned between two aluminum caps. The total length of the driver section from the bottom of the tube to the diaphragm measures 44.5 cm. Visualization of the evaporation is captured with a Phantom v12 camera operated at 29,200 fps and 1 μs exposure time with backlighting (high-power LED bank). The tube is placed inside of a square acrylic channel with water circulating with a large reservoir (water inlet and outlet on the bottom and top of the driver, respectively). Ice was added to the reservoir to maintain the

G. Ciccarelli (✉)
Queen's University, 130 Stuart Street, Kingston, ON, Canada
e-mail: ciccarel@queensu.ca

J. Melguizo-Gavilanes • J.E. Shepherd
California Institute of Technology, 1200 E. California Blvd,
Pasadena, CA, USA

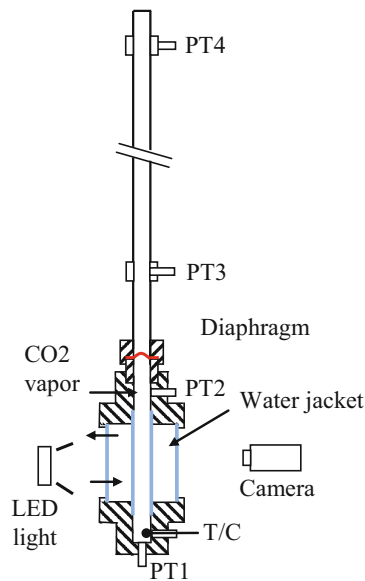


Fig. 1 Experimental setup

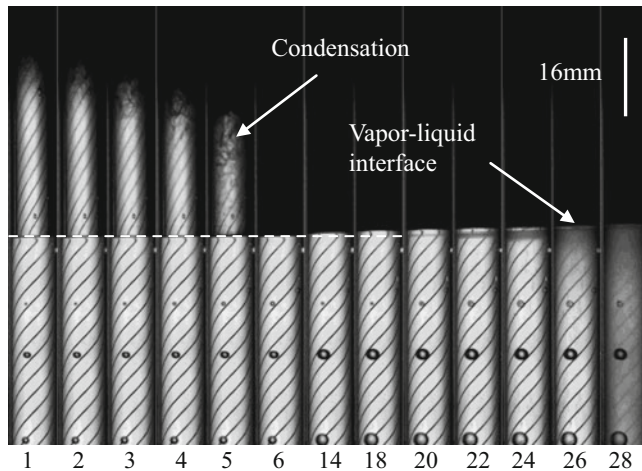


Fig. 2 Select video frames (test 53: 14.5 cm liquid CO₂ column height) showing the rising liquid surface following the interaction with the expansion wave: ($\Delta t_{\text{frame}} = 34.25 \mu\text{s}$)

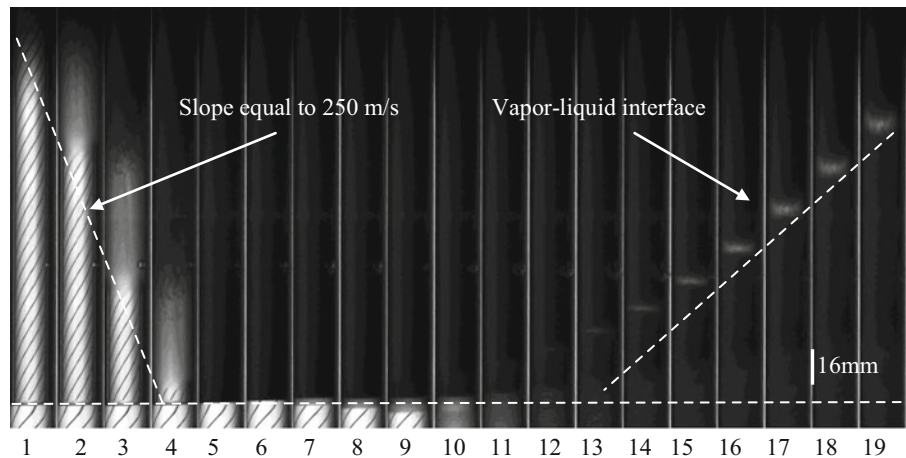
water temperature below 10 °C. The water surrounding the polycarbonate tube also reduces image distortion caused by the tube-wall curvature. The driven section consisted of a 1.16 m long, 16 mm inner-diameter stainless steel tube. The driven tube is connected to the driver assembly using a 3/4 in. stainless steel Swagelok VCR fitting. An aluminum diaphragm is used in the VCR fitting initially separating the CO₂ vapor and driven section of the shock tube. The 10 μm thick grade 1100 aluminum alloy used for the diaphragm consistently bursts between 4400 and 4500 kPa gauge (corresponding CO₂ saturation temperature of 11 °C), without the aid of an arrow point that would otherwise obstruct the expansion of the CO₂ into the driven section. In order to avoid restricting the expansion of the CO₂ the inner diameter of the VCR fitting after the diaphragm is drilled to 17 mm in order to accommodate the diaphragm thickness.

An experiment is started by loading solid CO₂ (dry ice) chunks into the driver through the top of the VCR fitting. Evolving CO₂ vapor purges all the air from inside the tube. The diaphragm is placed into position and the driven section is fastened to the driver via the VCR fitting. As the solid CO₂ heats up, it melts and collects at the bottom of the liquid layer that forms with a vapor space above. When the solid is completely melted, there is a large temperature gradient in the liquid column. A thermocouple at the bottom of the driver measures low temperatures around −30 °C. The driver pressure slowly rises as the liquid heats up and boiling occurs. When the diaphragm burst pressure is reached, rapid depressurization of the vapor volume is initiated, followed by the depressurization and boiling of the liquid column. At the time of diaphragm rupture, the bottom thermocouple measures a liquid temperature of 7–8 °C. During the slow pressurization, nucleation occurs at the tube wall filling the liquid column with rising vapor bubbles that burst at the surface creating a frothy liquid-vapor interface. In order to improve the initial conditions, CO₂ gas from a compressed gas cylinder was slowly added to the driver-section vapor space during the slow pressure rise (starting at a pressure of 3800 kPa). This suppressed the boiling at the time of diaphragm rupture producing quiescent liquid conditions. The height of the liquid column was varied and the pressure-time history following diaphragm rupture was recorded at four locations shown in Fig. 1 using PCB piezoelectric pressure transducers. The position of the pressure transducers relative to the driver end wall are PT1, 0 cm; PT2, 41.91 cm; PT3, 58.42 cm; and PT4, 140.34 cm. Following each test, the driven section is removed and the contents are purged with nitrogen gas; the initial driven-section pressure for all tests was 101 kPa.

Results

Figure 2 shows select video images taken of the driver section from a test with a 14.5 cm long column of liquid CO₂. The diagonal striped background is used for reference, and frame 1 is arbitrary assigned. In this test the diaphragm burst at a pressure of 4400 kPa. Several air bubbles attached to the outside of the tube are observed in the images that grow and shrink with system pressure changes. Following diaphragm rupture, an expansion wave propagates downward (not visible in Fig. 2) isentropically cooling the initially saturated vapor. A “condensation front” can be seen propagating down the tube. The front is not well defined, with rather spotty patches of droplets followed with the complete blocking of the backlight, probably caused by a more uniformly distributed mist. The expansion fan reflects off the liquid column surface, further dropping the pressure in the vapor, and continues to propagate through the liquid CO₂. A short time after the condensation front reaches the liquid surface, the liquid column height starts to increase

Fig. 3 Video frames (test 55) showing descending condensation wave and rising vapor-liquid interface (240 μ s between frames). Dotted lines are for reference only



indicating the start of phase change (the dotted horizontal line marks the initial interface height). From frame 20 the liquid becomes cloudy starting with a thin layer just below the initial interface height. This could be a result of the evaporation starting at the bottom of the meniscus. There is no discernable evaporation front observed past frame 24, as reported in Ref. [10], but rather an increase in the cloudiness caused by the generation of microbubbles throughout the column.

Figure 3 shows video images taken of the driver section from a test with a shorter 8.5 cm long column of liquid CO₂. The images show the condensation front propagating down the tube. Unlike in Fig. 2, the droplet region in the condensation front is preceded by a blurry region that propagates at a velocity of 250 m/s between frames 2 and 4, which is above the 200 m/s speed of sound in the CO₂ vapor [11]. It is unclear if this blurriness is associated with changes with CO₂ vapor or the contraction of the polycarbonate tube. After the expansion fan interacts with the liquid surface, the liquid-vapor interface starts to rise in frame 6, with phase change starting just below the liquid-vapor interface and spreading down through the column, as in Fig. 2. As observed by Tosse et al., the subsequent vapor-liquid interface (contact surface) is observed accelerating (the straight dotted line is just for reference) upward. The contact surface acts like a piston generating compression waves that influences the pressure distribution behind the shock wave generated after the diaphragm burst. The contact surface travels roughly one tube diameter between frames 18 and 19, giving a velocity of roughly 67 m/s.

The pressure-time history recorded by the four pressure transducers for a baseline test where the driver only contained CO₂ vapor (diaphragm burst at 4400 kPa) is shown in Fig. 4. Time zero for the pressure traces is arbitrary as there is no measurement of the burst time of the diaphragm. Following the diaphragm rupture, an expansion fan travels down the driver section causing the pressure at

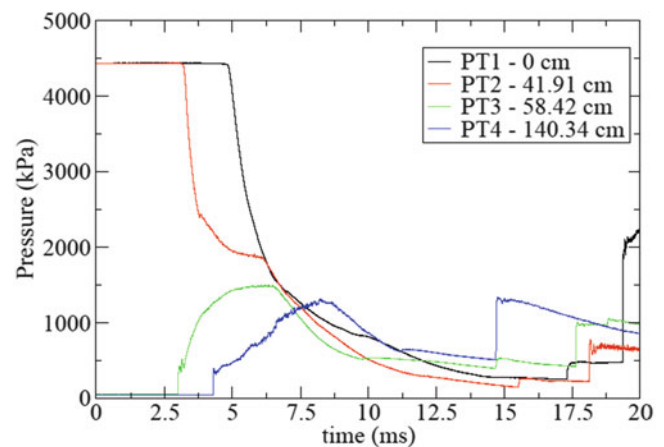
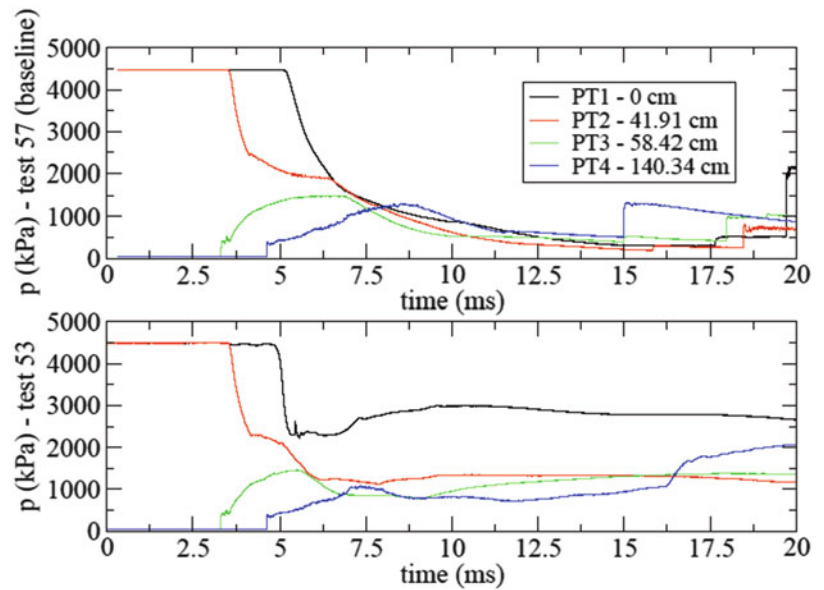


Fig. 4 Pressure histories for driver filled with CO₂ vapor only (test 57 – baseline)

PT2 (2.54 cm below the diaphragm) to drop precipitously, followed by a similar drop in pressure at PT1. Based on Fig. 4, the head of the expansion fan propagates from PT2 to PT1 in roughly 2 ms. This is consistent with the transducer separation distance of 41.9 cm and a CO₂ vapor speed of sound of 200 m/s [11]. The head of the expansion fan reflects off the driver end wall and propagates back up to the diaphragm position causing a second sudden pressure drop in the PT2 pressure trace at 6 ms. The very high initial pressure ratio across the diaphragm produces a supersonic expansion that results in a rising pressure at a fixed location downstream of the diaphragm position after the passage of the shock wave. The pressure at PT2 starts to decay at roughly 6.5 ms after the passage of the sonic point. Based on the time of arrival at PT3 and PT4, the shock velocity is 655 m/s (Mach 1.9). The shock wave reflects off the driven end wall reaching PT4 at 15 ms. Since PT4 is the pressure transducer nearest the end wall, the reflected shock pressure is highest there, decaying as it passes through the expansion fan at PT3.

Fig. 5 Comparison of pressure histories for liquid CO₂ column height of 14.5 cm in driver (test 53) versus CO₂ vapor only (test 57) same as Fig. 4



The pressure traces obtained for the 14.5 cm liquid CO₂ column height (corresponding video shown in Fig. 2) are provided in Fig. 5 (top). For comparison the pressure traces obtained with the driver completely filled with CO₂ vapor (shown in Fig. 4) are also provided. The time base for the pressure traces from the two tests is lined up based on the initial drop in pressure recorded at PT2 (associated with the arrival of the head of the expansion fan). The initial pressure drop at PT2 for both experiments is identical. The head of the expansion fan arrives at PT1 quicker in the test with the liquid since the speed of sound in the liquid column is faster than in the vapor. The higher speed of sound in the liquid also makes the pressure drop at PT1 steeper. The second drop in pressure recorded at PT2 occurs earlier for the test with the liquid because the liquid surface reflects the expansion fan, and therefore the round trip distance in the vapor is shorter. In the driver, the effect of the CO₂ evaporation is manifested in Fig. 5 by the leveling off of the pressure recorded at PT1 starting at 5 ms and the sudden pressure rise observed at 7 ms. A similar trend is observed in PT2. The CO₂ evaporation does not influence the shock wave or the initial pressure rise associated with the supersonic expansion at PT3 and PT4. The two-phase flow produced by the evaporation cuts short the pressure rise at PT3 (associated with the supersonic expansion), due to the earlier arrival of the sonic point at PT3. There is a slow pressure rise in PT3 and PT4 at later times that is not observed in the vapor-only pressure traces, top of Fig. 5. This pressure rise is caused by compression waves generated by the piston effect associated

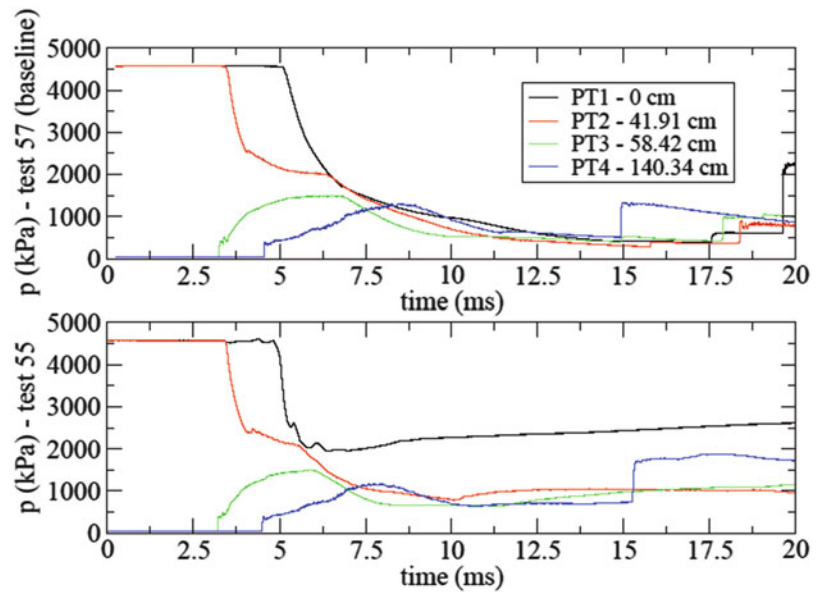
with the accelerating liquid-vapor interface observed in the images in Fig. 3. The two-phase flow makes the pressure rise recorded at PT4 associated with the reflected shock wave slower than for the vapor-only case.

The pressure traces obtained for the 8.5 cm liquid CO₂ column height (video shown in Fig. 3) are provided in Fig. 6. All the observations made concerning comparison of the 14.5 cm liquid column and the vapor-only results described in reference to Fig. 5 also apply to the shorter liquid column height, results shown in Fig. 6. The effects are not as strong since the height of the vapor space is larger, and so the effects of the liquid are delayed and muted. One of the noticeable differences is that the pressure rise associated with the reflected shock wave at PT4 is steep indicating that the two-phase mixture does not reach PT4.

Conclusions

High-speed video taken of the driver section shows that the expansion process involves a condensation front that propagates through the vapor, followed by evaporation of the liquid that produces a two-phase flow delineated by a contact surface that travels upward. The motion of the contact surface produces compression waves that have a strong effect on the post-shock pressure profile. The rapid evaporation has no effect on the initial stage of the driver expansion which is governed by the vapor expansion but ultimately keeps the driver at an elevated pressure for an extended period of time.

Fig. 6 Comparison of pressure histories for liquid CO₂ column height of 8.5 cm in driver (test 55) versus CO₂ vapor only (test 57) same as Fig. 4



References

- Ciccarelli, G., Frost, D.L.: Fragmentation mechanisms based on single-drop experiments using flash x-ray photography. *Nucl. Eng. Design* **146**, 109–132 (1994)
- Voort, M.M., Berg, A.C., Roekaerts, D.J., Xie, M., Bruijn, P.C.: Blast from explosive evaporation of carbon dioxide: experiment, modeling and physics. *Shock Waves* **22**, 129–140 (2012)
- Reid, R.C.: Superheated liquids. *Am. Sci.* **64**, 146–156 (1976)
- Reid, R.C.: Possible mechanisms for pressurized-liquid tank explosions or BLEVE's. *Science* **203**, 3 (1979)
- Shepherd, J.E., Sturtevant, B.: Rapid evaporation at the superheat limit. *J. Fluid Mech.* **121**, 379–402 (1982)
- Frost, D.L.: Dynamics of explosive boiling of a droplet. *Phy. of Fluids* **31**(9), 2554–2561 (1988)
- Hill, L.G.: An experimental study of evaporation waves in a superheated liquid. Dissertation (Ph.D.), California Institute of Technology, (1990)
- Simoës-Moreira, J.R., Shepherd, J.E.: Evaporation waves in superheated dodecane. *J. Fluid Mech.* **382**, 63–86 (1999)
- Kuznetsov, V.V., Kozulin, I.A., Vitovsky, O.V.: Experimental investigation of adiabatic evaporation waves in superheated refrigerants. *J. Eng. Thermophy.* **21**(2), 136–143 (2012)
- Tosse, S., Vaagsaether, K., Bjerketvedt, D.: An experimental investigation of rapid boiling of CO₂. *Shock Waves* **25**(3), 277–282 (2015)
- Span, R., Wagner, W.: A new equation of state for carbon dioxide covering the fluid region from the triple-point temperature to 1100 K at pressures up to 800 MPa. *J. Phys. Chem. Ref. Data* **25**, 1509–1596 (1996)